Journal of Earth and Atmospheric Research

STOCHASTIC SEISMIC INVERSION FOR RESERVOIR CHARACTERIZATION IN 'BRIGHT' FIELD, NIGER DELTA

[1]Abe, J. S. [2]Olowokere, M. T. [3]Enikanselu, P. A.

[1,2,3]Department of Applied Geophysics, The Federal University of Technology Akure

Article History
Received: 01-01-21
Accepted: 22-09-21

Keywords:
Deterministic inversion, Acoustic impedance, Realization, Horizon

ABSTRACT

Subsurface characterization is key to the success of any oil exploration work and this task requires the integration of several techniques to be able to capture subsurface heterogeneity properly. Inversion sections normally have a lot of uncertainties in them which have direct impact on any exploration and exploitation work. The stochastic or probabilistic approach is very important because the uncertainties in inversion sections are catered for. This research work involves the use of 3D seismic volume and suite of well logs in 4-wells to characterize the reservoirs in the field. The approach used includes petrophysical analysis, seismic interpretation and stochastic inversion. Two sand bodies were mapped across the entire field showing their geometry and lateral continuity, gamma ray and resistivity logs were used to delineate the reservoirs prior to correlation and relevant equations were used to estimate the reservoir parameters. Seismic to well tie was done to enable proper picking of the horizons and generation of structural maps, Deterministic seismic inversion was then carried out using the three wells, horizons and the seismic section and thereafter stochastic inversion was done to obtain three realization volumes. The P-Impedance, density, porosity and Vp/Vs ratio in the 3D models indicated the presence of hydrocarbon within the mapped reservoirs. The deterministic inversion sections along the structures also showed favourable impedance values within the reservoirs of interest and the stochastic inversion result displayed variation in acoustic impedance across the sections in the three realizations generated.

Correspondence:jsabe@futa.edu.ng

1.0 INTRODUCTION

Seismic inversion involves extracting from seismic data, the underlying geology that gave rise to the seismic (Russell, 2005). This is done by deriving impedance from seismic data, which is an interval property useful for estimating properties such as porosity. Inversion is actually an inverse forward modeling process (Ghosh, 2013).

Seismic inversion works as an important means to estimate subsurface parameters in reservoir geophysics, which plays an important role in lithology prediction and geofluid discrimination (Castagna 2001; Buland and Omre, 2003; Russellet al.2003, 2011;Downton, 2005; González *et al*., 2008; Zhang *et al*., 2012; Zhang, 2017;Yin and Zhang 2014;Yin *et al*., 2015; Connolly and Hughes 2016; Aleardi, 2018; Feng *et al*. 2018). Due to the bandlimited characteristics (i.e. lack of low- and high frequencies) and strong ill-posedness of seismic inversion (Yin *et al*., 2016, 2017;Li *et al*., 2017, 2019), the stability, uncertainty and resolution of

seismic inversion are the eternal research topics that geophysicists have been discussing for many years.

In addition to the routine interpretation of well and seismic data, inversion will further assist in proper characterization of our hydrocarbon bearing reservoirs. The interest in seismic inversion techniques has been growing steadily over the last couple of years. Integrated studies are essential to hydrocarbon development projects (Vazquez *et al*., 1997, Cosentino, 2001) and inversion is one of the means to extract additional information from seismic data. Inversion replaces the seismic signature by a blocky response, corresponding to acoustic and/or elastic impedance layering. It facilitates the interpretation of meaningful geological and petrophysical boundaries in the subsurface (Gunning, 2004).

Inversion increases the resolution of conventional seismics in many cases and puts the study of reservoir parameters at a different level. It results in optimised volumetrics, improved ranking of leads/prospects, better delineation of drainage areas and identification of 'sweet spots' in field development studies (Veeken *et al*. 2002). The inversion methods are either deterministic or probabilistic and the approach can be post- and/or pre-stack. Inversion schemes generally use migrated time data as basic input. The pre-stack method exploits AVO effects on migrated CDP gathers.

All modern seismic inversion methods require seismic data and a wavelet estimated from the data. Typically, a reflection coefficient series from a well within the boundaries of the seismic survey, is used to estimate the wavelet phase and frequency. Accurate wavelet estimation is critical to the success of any seismic inversion (Schlumberger 2008). The inferred shape of the seismic wavelet may strongly influence the seismic inversion results and, thus, subsequent assessments of the reservoir quality. Wavelet amplitude and phase spectra are estimated statistically from either the seismic data alone or from a combination of seismic data and well control using wells with available sonic and density logs. After the seismic wavelet is estimated, it is used to estimate seismic reflection coefficients in the seismic inversion.

In general there are two types of inversion, deterministic and stochastic. Deterministic inversion is relatively straightforward to generate and is based on the minimisation of the difference between a modelled seismic trace and the actual seismic trace (Latimer et al. 2000). As such, these types of inversion is smoothed solutions, representing a best estimate within the limits imposed by the bandwidth of the data. This effectively means that in areas where the geology is layered on a scale less than about 1/4 of the seismic wavelength the resulting inversion is likely to be inappropriate for quantitative interpretation. Unfortunately, this scale is important in most reservoirs.

The non-uniqueness of the sub-tuning component in seismic can be addressed through stochastic inversion, which uses geostatistics to generate multiple impedance realisations, at the reservoir model scale (Moyen and Doyen, 2009). Each realisation matches the seismic trace, honours the statistics of property variation between well data points and ties the wells exactly. Realisations can be transformed to reservoir properties (using rock physics relationships and various mapping algorithms) and the results can be analysed in terms of uncertainty as well as connectivity. These types of stochastic inversion products are invaluable for conditioning geomodels in reservoir development but there is usually a significant cost in time and money to produce them.

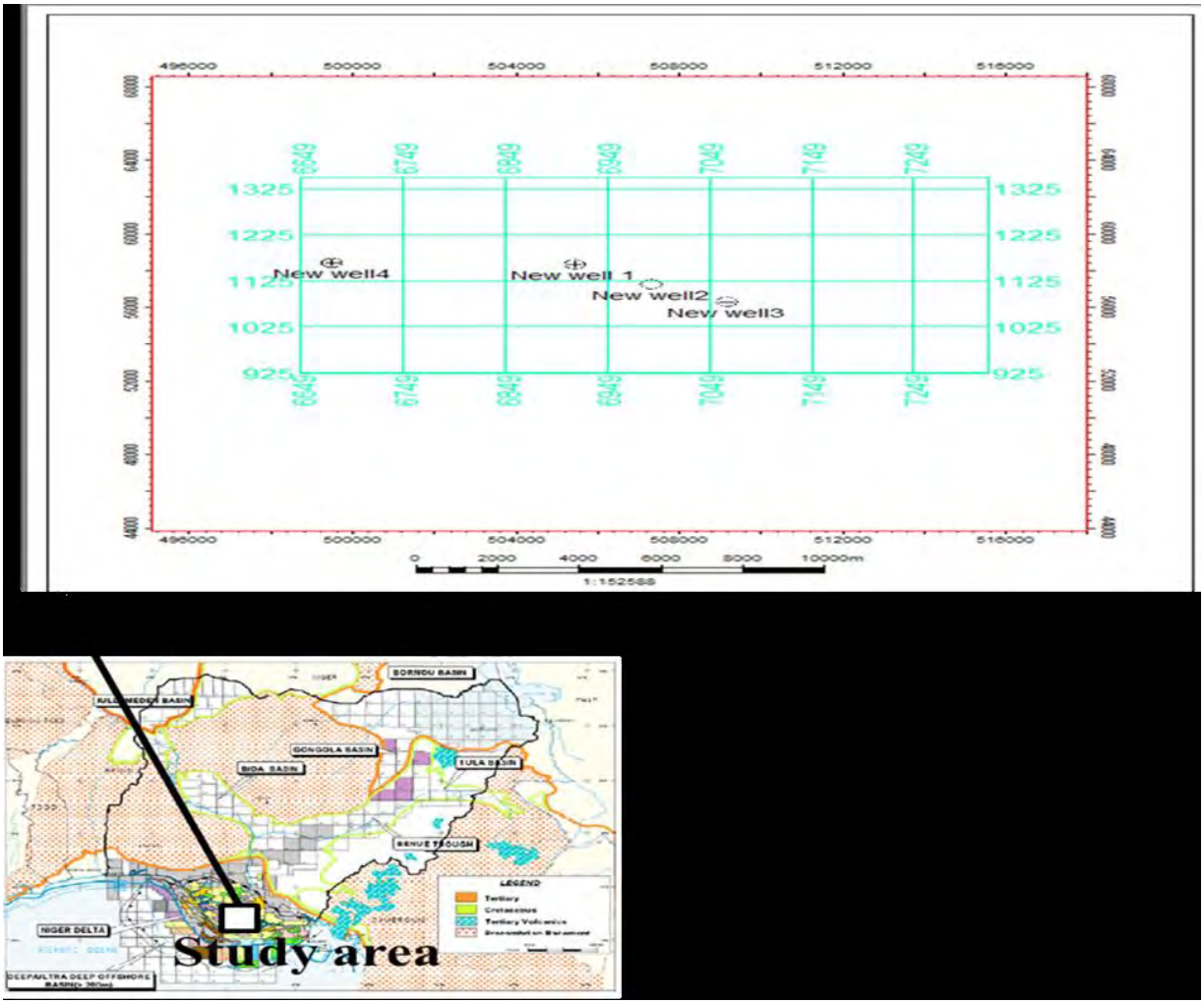


Figure 1: *Base Map and Map of Nigeria showing the study area*

Location and Geology of the Study Area

The field is located within the onshore part of Niger delta. (Figure 1). The base map showed the location of the four wells and the seismic lines, a total of 673 inlines and 425 crosslines were interpreted. The field belongs to an active oil producing company in Nigeria. It covers an area extent of about 51,187 km^2 and it lies within longitude 8.0°E to 8.3°E and latitude 4°N to 4.3°N .

Niger Delta basin is bounded by the geographical grids of latitudes 6° 40'E and longitudes 8° 30'N. It contains mainly Cenozoic formations deposited in high energy constructive deltaicenvironments as differentiated into continental Benin, paralic Agbada, and pro-delta marine Akata facies (Doust and Omatsola, 1990, Short and Stauble, 1967). The Benin Formation (Figure 2) is the upper alluvial coastal plain depositional environment of the Niger Delta Complex. It extends from the west Niger Delta across the entire Niger Delta area and to the south beyond the present coastline. The formation was deposited in a continental fluviatile environment and composed almost entirely of non-marine sandstone. It consists of coarse-grained sandstones, gravel lignite streaks and wood fragments with minor intercalation of shales. Benin Formation is of Miocene to younger age and has a variable thickness that exceeds 1820 m. In the subsurface, it is of Oligocene age in the

north becoming progressively younger southwards but ranges from Miocene to Recent as generally accepted. Very little hydrocarbon accumulation has been associated with this formation (Short and Stauble, 1967). The Agbada Formation underlies the Benin Formation. It was laid down in paralic brackish to marine fluviatile, coastal environments. It is made up mainly of alternating sandstone, silt and shale. The sandstones are poorly sorted, rounded to sub-rounded, slightly consolidated but majority are unconsolidated. The sandstones grade into shale in the lower part of the formation. Agbada Formation ranges in age from Eocene in the north to Pliocene in the south. The sandy parts of the formation are known to constitute the main hydrocarbon reservoirs of the delta oil fields and the shales constitute seals to the reservoirs. The thickness of the formation reaches a maximum of about 4500 m (Short and Stauble, 1967). The

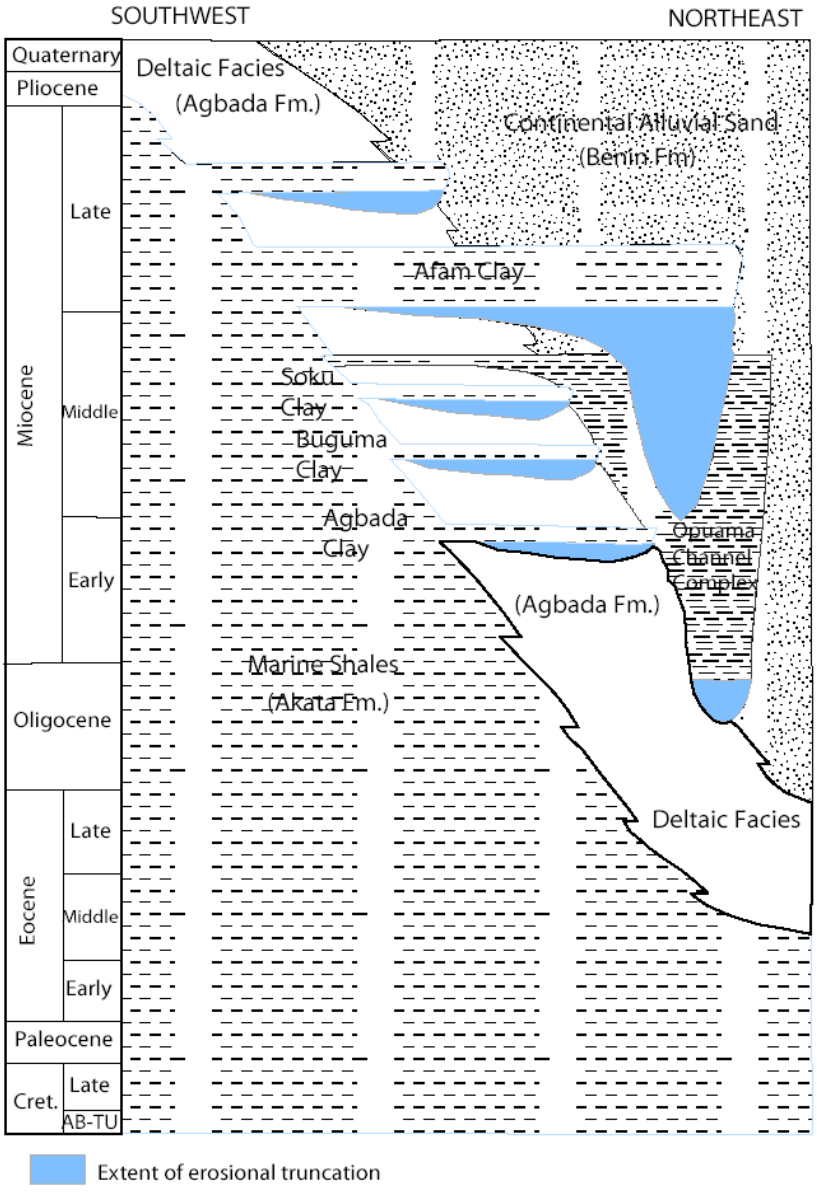


Figure 2: *Stratigraphic column showing the three formations of the Niger Delta. Modified from Doust and Omatsola (1990)*

Akata Formation is the lowest unit of the Niger Delta complex. It is composed of mainly shale with sandstones and siltstones locally interbedded. The Formation becomes shalier with depth. It was deposited in a marine environment and has a thickness, which may reach 7000 m in the central part of the delta. The Akata Formation outcrops offshore in diapirs along the continental slope, and onshore in the north east, where they are called Imo Shale. The age of the Akata Formation ranges from Eocene to Recent (Short and Stauble, 1967).

2.0 Methodology

The method adopted for this research work began with reservoir delineation from well logs and subsequent mapping of horizons from seismic sections to generate time and depth structural maps. This serves as input to the seismic inversion workflow. The seismic inversion workflow used for this research work is stated below:

Wavelet Extraction: The inversion process involved extracting a statistical wavelet which was removed from the seismic trace in order to obtain the real earth model (acoustic impedance). The wavelet extracted was zero phase and the frequency, about 25 Hertz.

Correlation of Wells: This involved linking the events on the seismic and the synthetic to ensure that there was a perfect tie between peak to peak and trough to trough. A correlation coefficient value of over 0.5 was obtained to generate a good model.

Strata Model Building: Initial models of P-impedance, velocity, density, Vp/Vs were then generated to view the variation of these properties on the entire seismic volume(inlines and crosslines). Since it was a model based inversion, this initial model was necessary for the actual inversion.

SI Model Building: This was the initial seismic inversion (deterministic inversion). The inputs into this were the seismic horizons, wells and the estimated wavelet. The deterministic inversion result showed the variation of P-Impedance along the structure (mapped horizons).

Wavelet Scaling with Strata Model and Seismic: Because of the differences in wavelet scaling of the seismic and model there is need to synchronize the scales.

Variogram Analysis: This was done to obtain the statistical parameters needed to obtain values for the unknown points especially to distribute spatial data. The sequential Gaussian Simulation was the algorithm used to obtain various realizations and possibilities of inversions.

Stochastic inversion: This was the actual stochastic inversion that is meant to generate several realizations of the initial deterministic inversion result. The inputs were the initial models, horizons, wells and variogram. The process was time- consuming, as it took hours or days. Three realizations were generated and interpreted in this research.

3.0 Results and Discussion

Inversion involves obtaining the earth model or the acoustic impedance from seismic data which in turn involves estimating statistical wavelet as shown in Figure 3. It is a zero phase wavelet because it is symmetrical at the origin. Its frequency is about 25Hertz. Only three wells were used to run the inversion because Well 3 had no density log which is key to the inversion process. Four horizons were picked which properly captured the interval of interest.

The inversion was carried out on a different software, Hampson Russell which necessitated loading of data and correlation of events on the seismic and synthetics as shown in Figure 4. Correlation of wells is the process of adjusting the

depth/time relationship for each well to ensure that the calculated synthetics align optimally with the corresponding seismic data. The Log Correlation display shows a very accurate correlation between the synthetic traces (in blue) and the real composite trace (in red). The cross-correlation curve (upper right) confirms that there is no residual time-shift or phase error and a correlation coefficient of 0.612 was obtained before proceeding with the inversion process.

Since it is a model- based inversion, velocity, density, P-Impedance and Vp/Vs models were generated to view the way these properties vary across the seismic volume and along well locations. The inputs that went into it are the horizons, wells and seismic section. Figure 5 is the strata model of velocity showing the variation of velocity across the section, location of Well 1 and the two Sands 1 and 2 previously analysed petrophysically and structurally. P-wave velocity within the hydrocarbon -bearing reservoir was observed to be comparatively low with respect to the overlying and underlying strata (shale), since a good reservoir will be porous and permeable and if the porosity is high then the velocity will be low.

Sands 1 and 2 in Well 1 (Figure 5) have low velocity indicated by the yellow colour within red from the colour bar. The velocity range within Sands 1 and 2 varied from 2550 m/s to 3016 m/s compared to the overlying and underlying strata with a range of velocity 3389 m/s to 3949 m/s.

The strata model of density (Figure 6) displays the variation of density within the section. The density values in the entire model varied from 1.98 to 2.47, while the density values in well 1, within Sand 1, varied from 2.29 to 2.31 and Sand 2 is 2.24 to 2.26. The density value in a typical hydrocarbon- bearing reservoir is expected to be low, because an increase in porosity within a good reservoir will cause a reduction in density. The

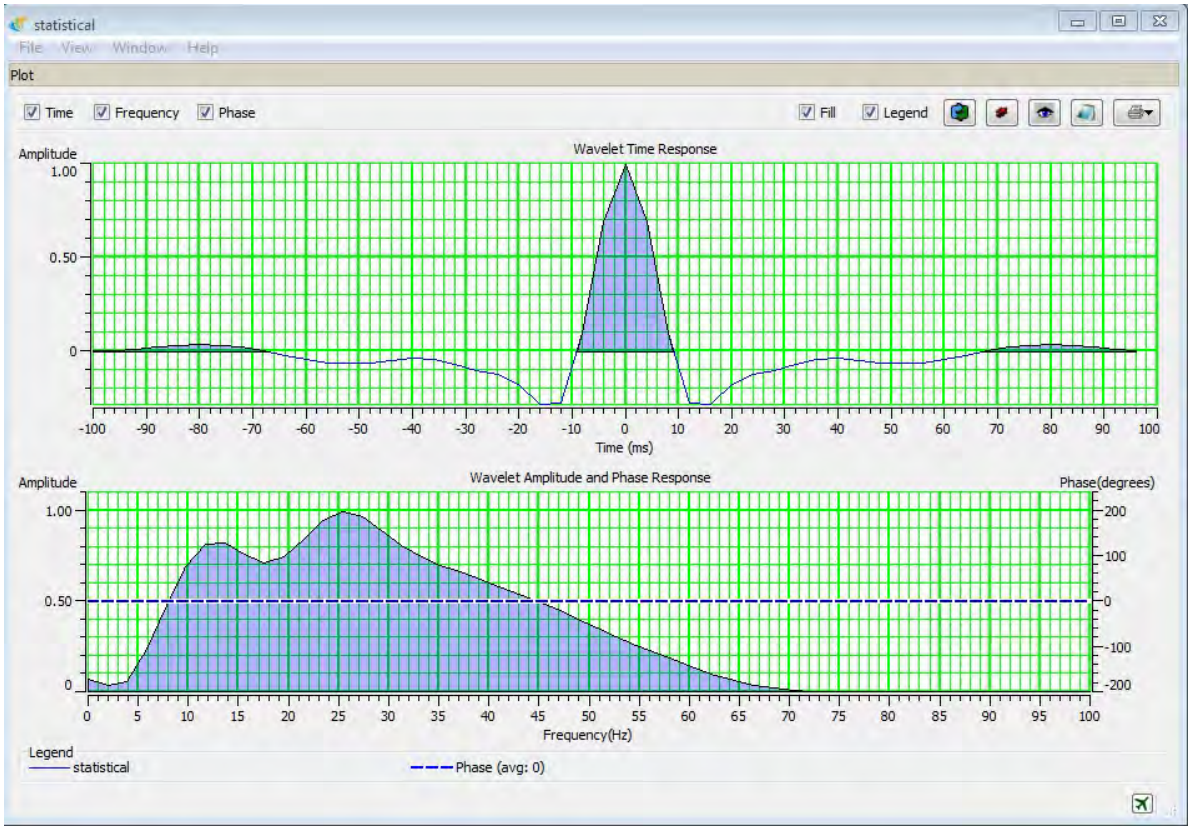


Figure 3: *Statistical Wavelet Extracted for Inversion*

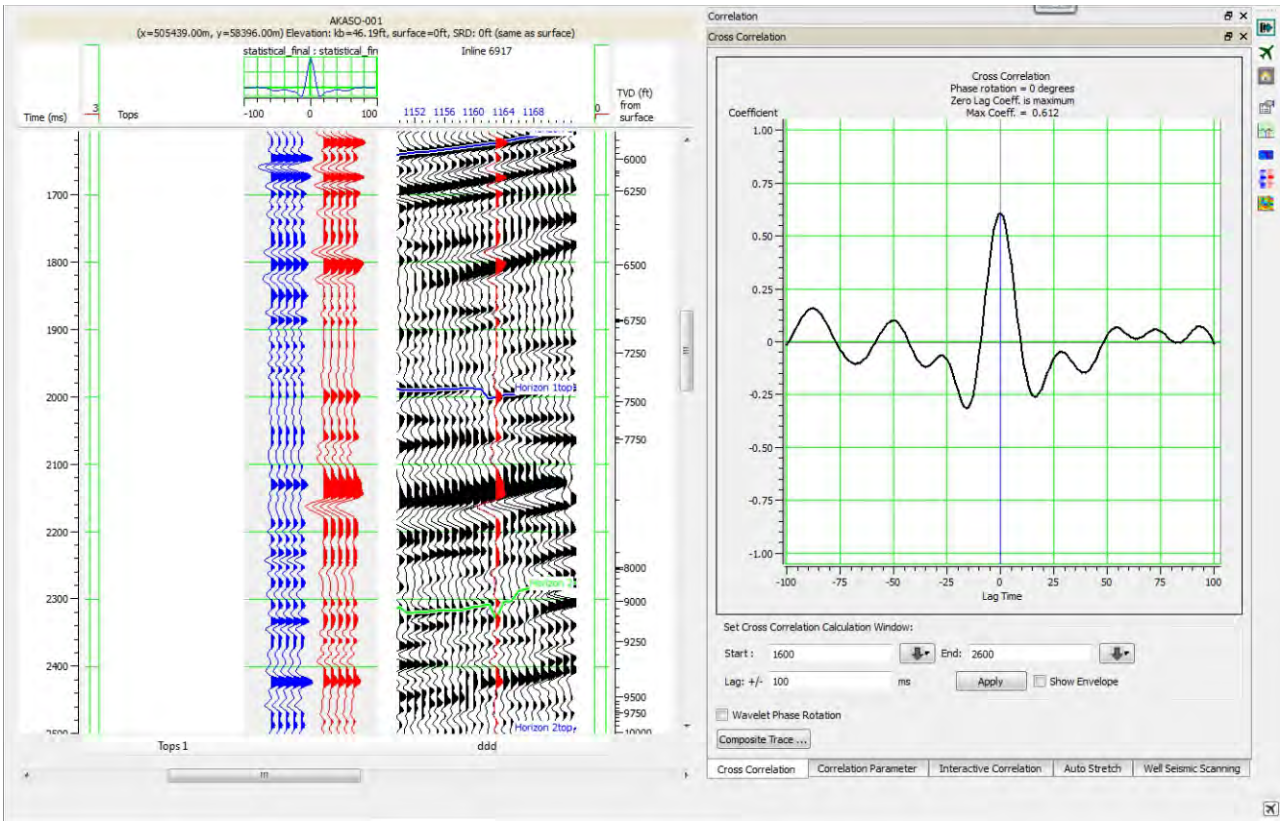


Figure 4: *Synthetic Seismogram for Event Matching*

density of sand 2 is lower than that of sand 1 because of the fluid in it.

Figure 7 shows the strata model of P-Impedance depicting the change in acoustic impedance within the section. Impedance is the product of density and velocity, while P-Impedance is the product of P-wave velocity and density. Within the hydrocarbon-bearing reservoir the value is expected to be low because of the low density and velocity values as established in Figures 6 and 7. Sands 1 and 2 have lower impedance values than the overlying and underlying strata. The range of P-impedance values within Sands 1 and 2 was from 6500m/s*g/cc to 7083m/s*g/cc against 7500 m/s*g/cc to 8083 m/s*g/cc in the overlying and underlying layers.

The strata model of Vp/Vs in Well 1 is also shown in Figure 8 with Sands 1 and 2 that were mapped. The Vp/Vs values within Sand 1 and Sand 2 ranged from 1.97 to 2.23 which is consistent with what is expected in the Niger Delta. This further validated the fact that Sands 1 and 2 are hydrocarbon-bearing due to the observed low values of velocity, density, P-Impedande and Vp/Vs.

With the initial models in place, the seismic inversion model will be built which is actually the deterministic inversion. The input is the existing strata model, the horizons were classified into zones to show the variation of P-Impedance only within the picked horizons. The deterministic inversion result on crossline 1163 is shown in Figure 9 with Well 1 and Well 4. Sands 1 and 2 are as shown along Well 1 .The impedance seems to be increasing from the top to the bottom of the section with some variations. The impedance values within Sands 1 and 2 along Well 1 are lower than the overlying and underlying layers. The values at the intervals of interest is from 6000m/s*g/cc to 6800m/s*g/cc compared to that

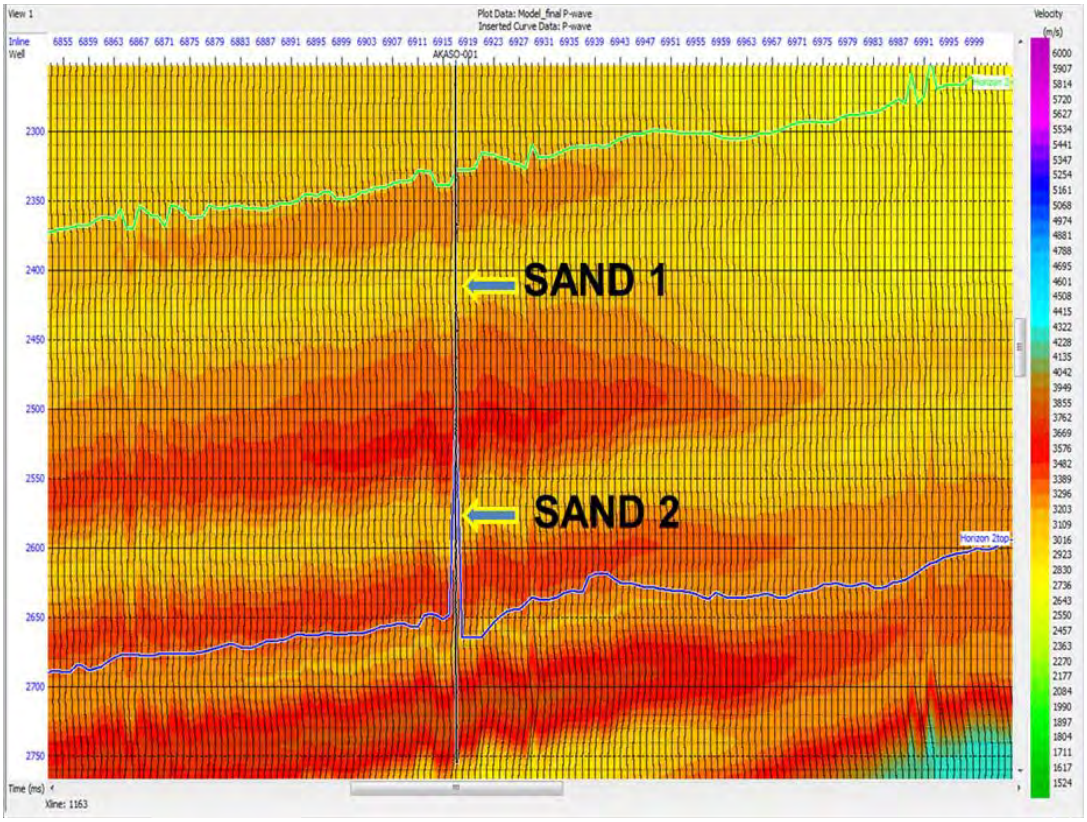


Figure 5: *Strata Model of Velocity on Inline 6917*

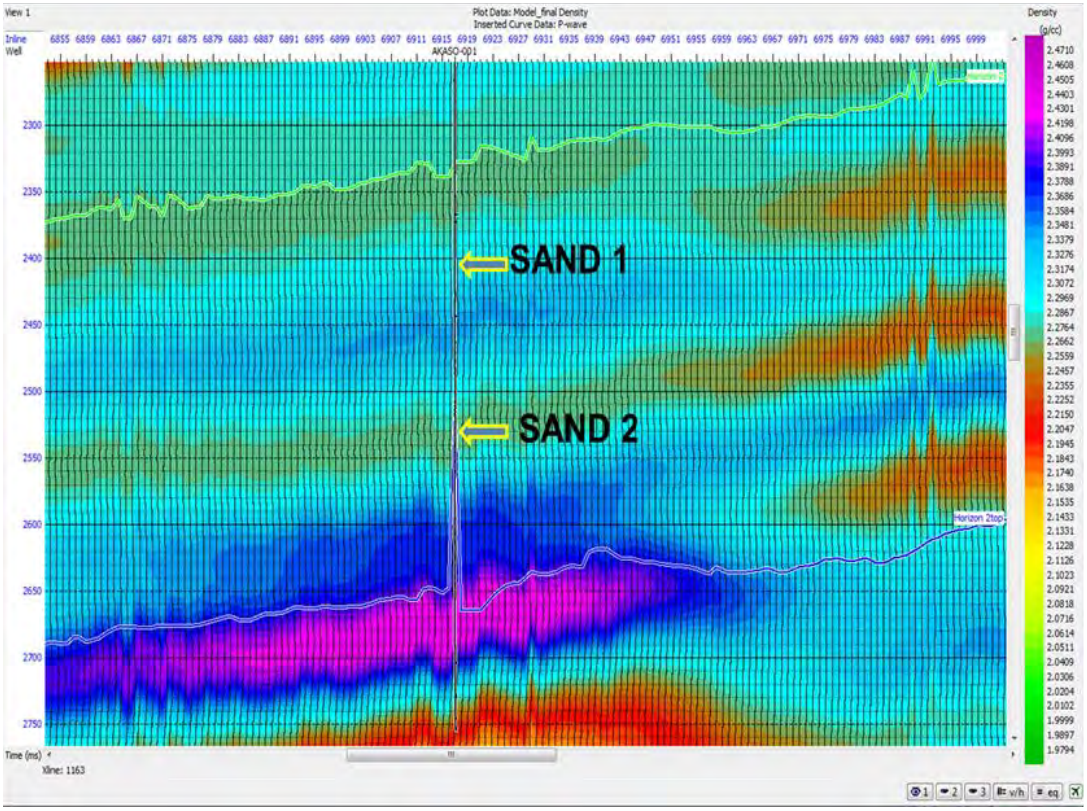


Figure 6: *Strata Model of Density on Inline 6917*

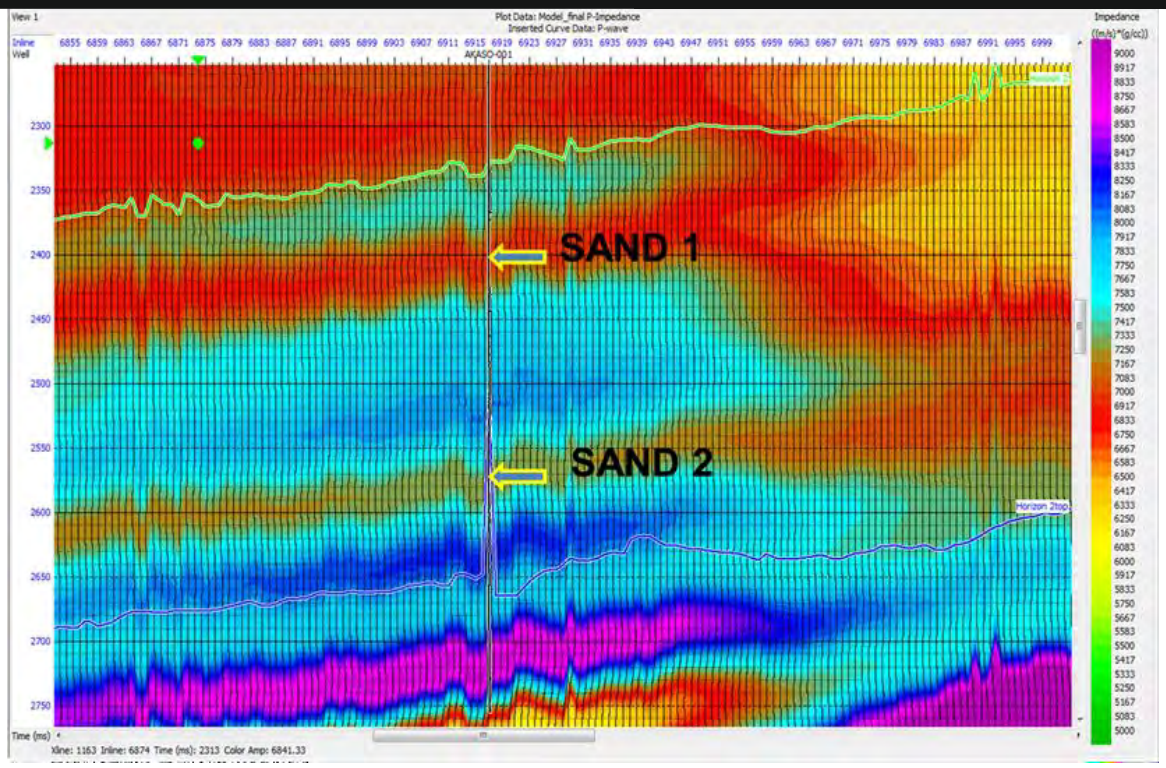


Figure 7: *Strata Model of P-Impedance on Inline 6917*

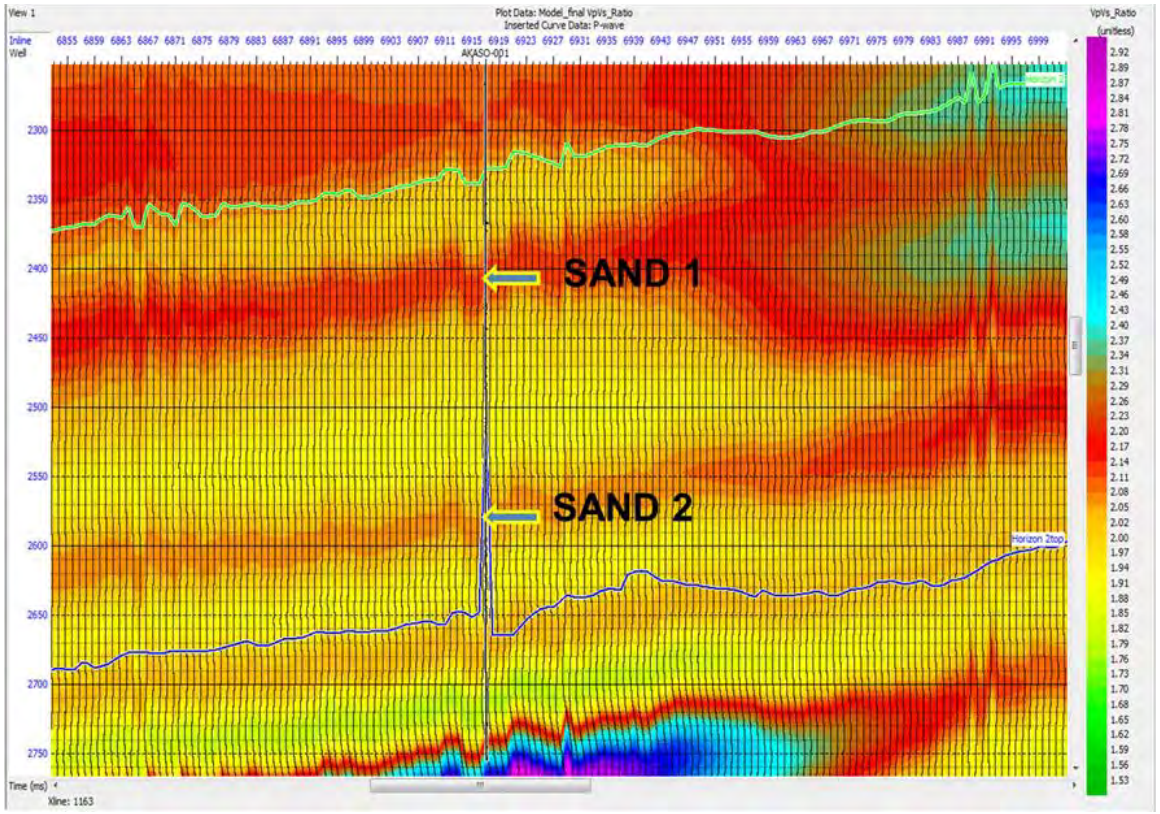


Figure 8: *Strata Model of Vp/Vs on Inline 6917*

above and below them, and Sand 2 seems to extend from one end of the section to the other at two way time of 2800ms. The deterministic inversion result on inline 6917 is shown in Figure 10 and the impedance values within Sands 1 and 2 are close to the values obtained from crossline 1163. The two mapped sands are continuous across the section. The impedance values at the top of the section are lower than the ones below, but there exceptions where we have low impedance layers within higher ones and this could be as a result of fluids (oil or gas) within it. Due to the difference in wavelet scaling between the strata model and seismic, there is need to synchronize the scales in other to generate a reliable stochastic inversion result. Figure 11 shows the result of wavelet scaling between the strata model and seismic where there is a good overlay between the time, frequency and phase responses and the wavelets are still zero phase. In other to populate data away from well locations and generate several realizations of the inversion sections which is the actual stochastic inversion there is need to carry out variogram analysis as shown in Figure 12, the variogram parameters used to perform the stochastic inversion are as follows: nugget is 0, sill is 1, spherical variogram model type was used and the x and y range is 1000.

Prior to running the stochastic inversion process on RokDoc, surface maps that show the variation of acoustic impedance across the surface close to Sands 1 and 2 were generated as shown in Figures 13 and 14. The acoustic impedance depth slice map close to Sand 1 shows the variation of the property on the map with the location of the three Wells 1, 2 and 4. The acoustic impedance at Well 1 is 5099m/s*g/cc, Well 2 is 6162m/s*g/cc and well

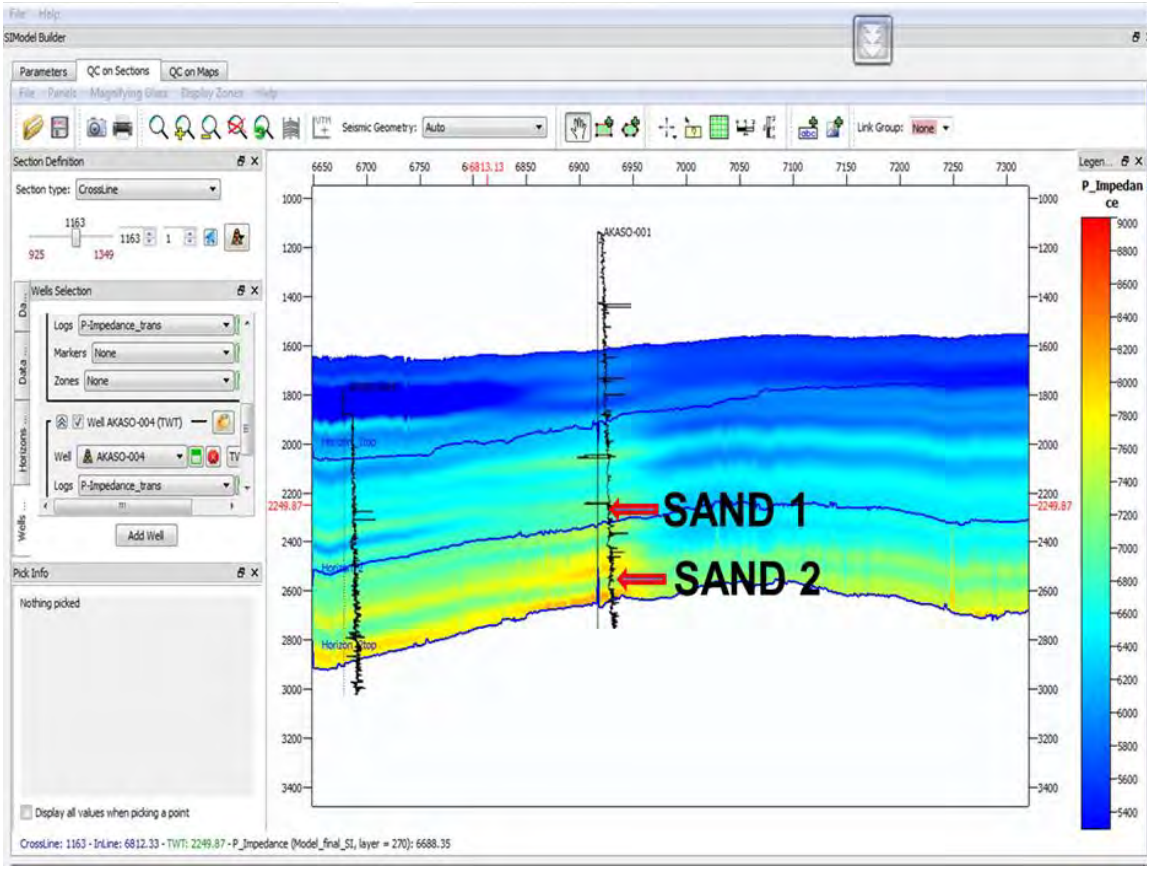


Figure 9: *Seismic inversion Model (Deterministic) on Crossline 1163*

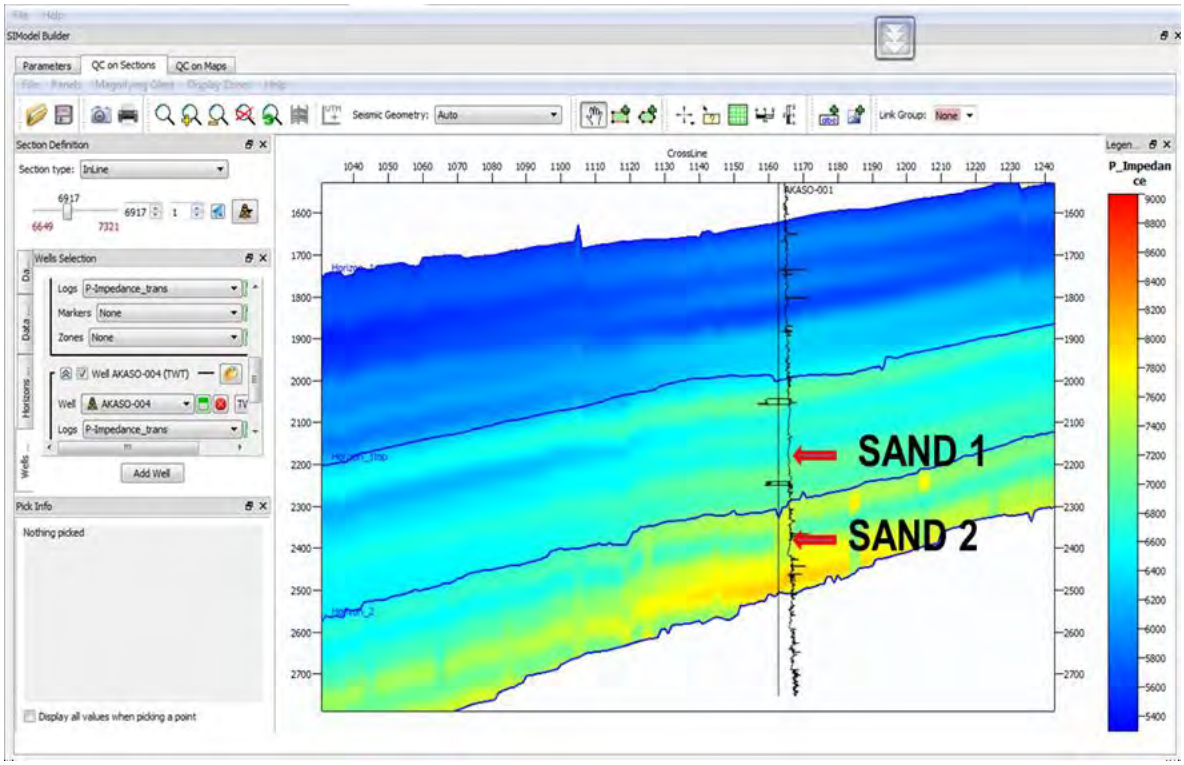


Figure 10: *Seismic inversion Model (Deterministic) on Inline 6917*

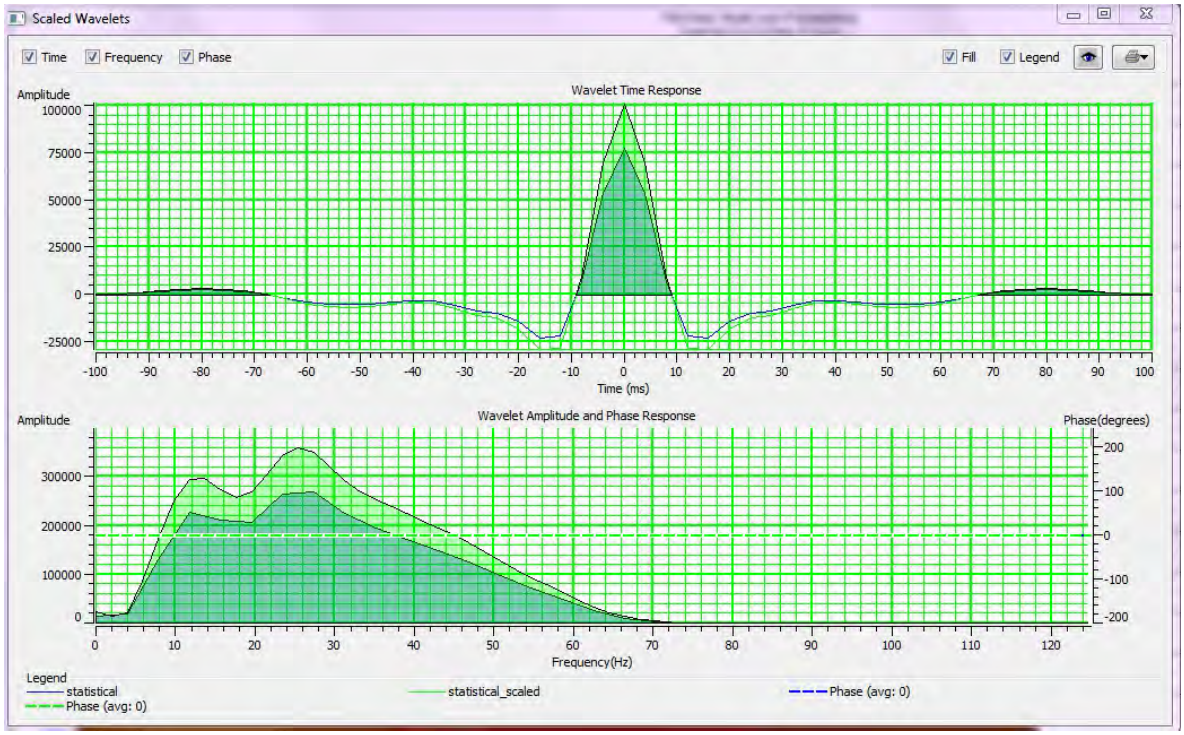


Figure 11: *Wavelet Scaling with Strata and Seismic*

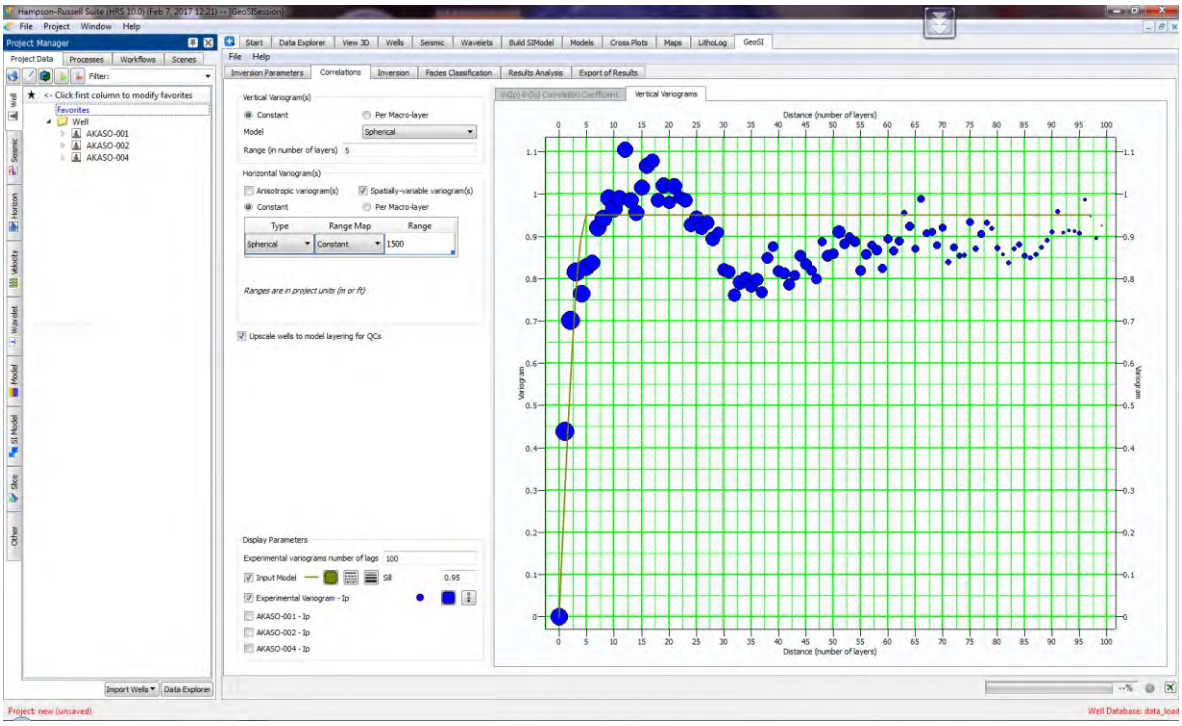


Figure 12: *Variogram Analysis for Inversion*

4 is 6370m/s*g/cc, however there are areas of higher acoustic impedance on the surface.

Figure 14 shows the variation of acoustic impedance on the surface and at well locations. The impedance values at the location of Well 1 is 7194m/s*g/cc, Well 2 is 6667m/s*g/cc and Well 4 is 6589m/s*g/cc, however there are other areas with lower acoustic impedance which could be due to the presence of hydrocarbon or unconsolidated materials and higher acoustic impedance which could be as a result of consolidated or compacted sediments.

The initials models and the variogram parameters were used as inputs for the stochastic inversion, three realizations were generated for the inline and crossline respectively. The first realization of stochastic inversion on inline 6917 shown in Figure 15 depicts the variation of this property on the section. The impedance values at well location vary from about 6000m/s*g/cc to 8500m/s*g/cc and the values at the mapped Sands 1 and 2 are low and there is a gradational increase in acoustic impedance from the top to the bottom of the seismic section. This is different from the second and third realizations in Figures 16 and 17. Higher acoustic impedance values are more evident in the second and third realizations compared to the first which shows the heterogeneity that exist within the subsurface which allow the language of probability in the prediction of reservoir parameters and assessment of risk and quantification of uncertainties (Falebita, 2011). The acoustic impedance at the crooslines and inlines locations at different two way time values are different. For example at 2400ms inline 6917 and crossline 1325, the impdeance value is highest in the first realization, lower in the second realization and increase a bit in the third realization.

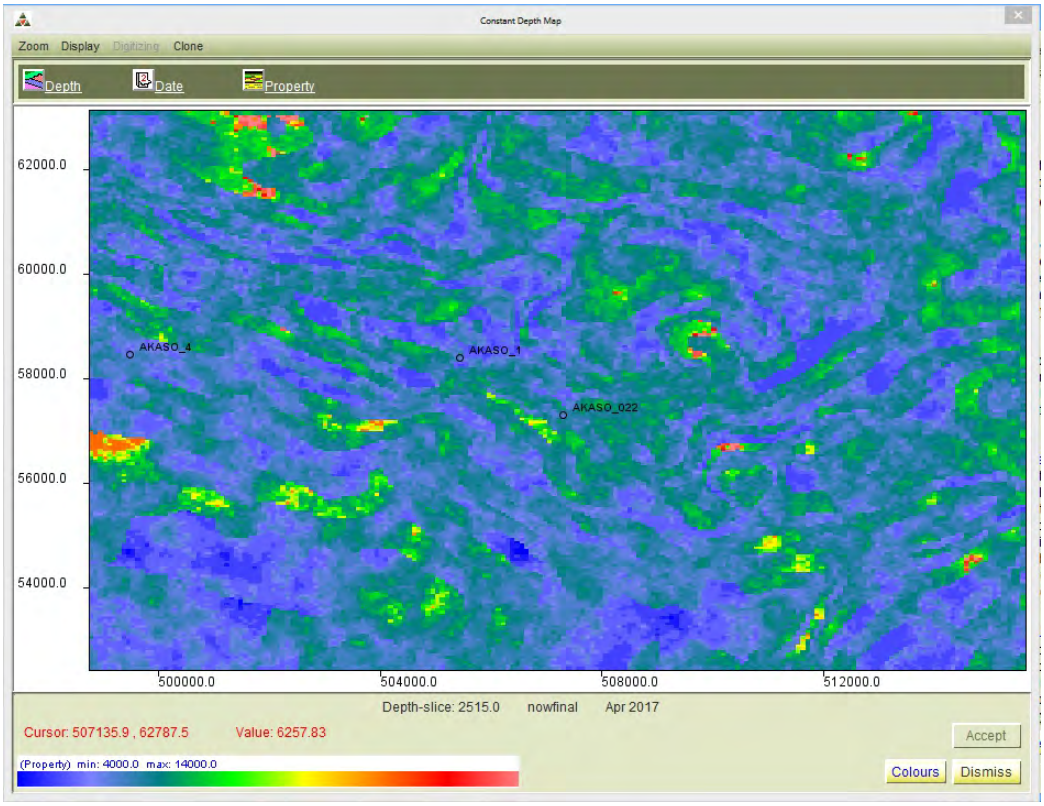


Figure 13: *Acoustic Impedance Variation Close to Surface Map of Sand 1*

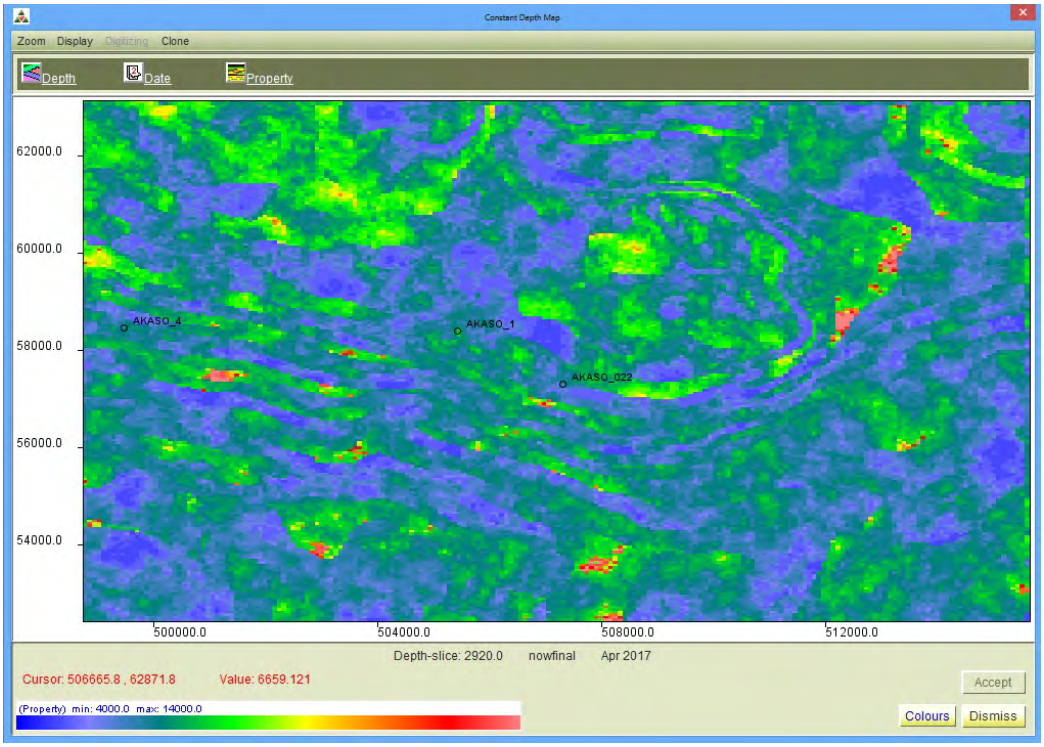


Figure 14: *Acoustic Impedance Variation Close to Surface Map of Sand 2*

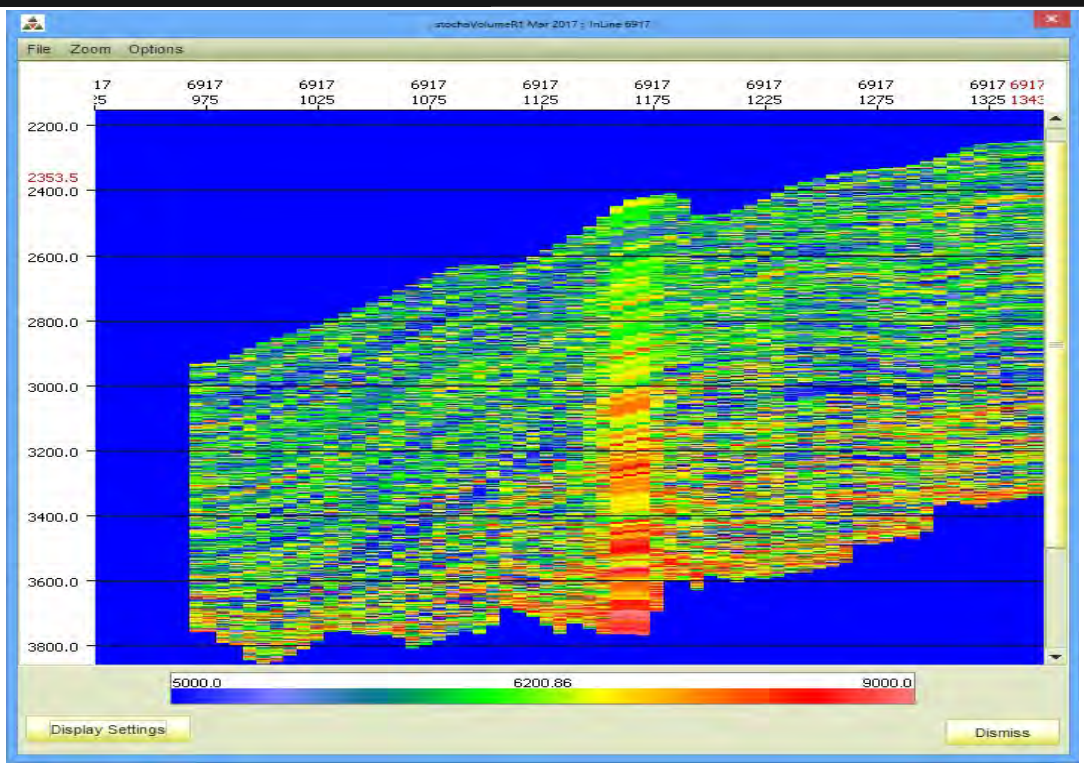


Figure 15: *1st Realization of Stochastic Inversion on Inline 6917*

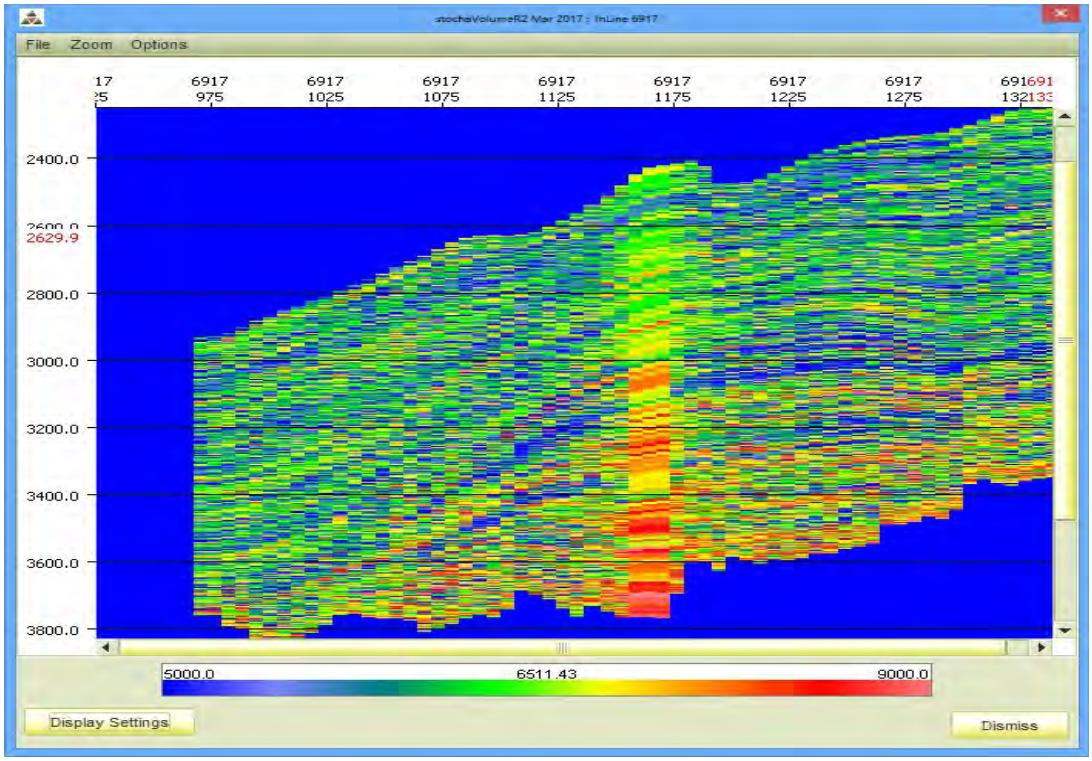


Figure 16: *2nd Realization of Stochastic Inversion on Inline 6917*

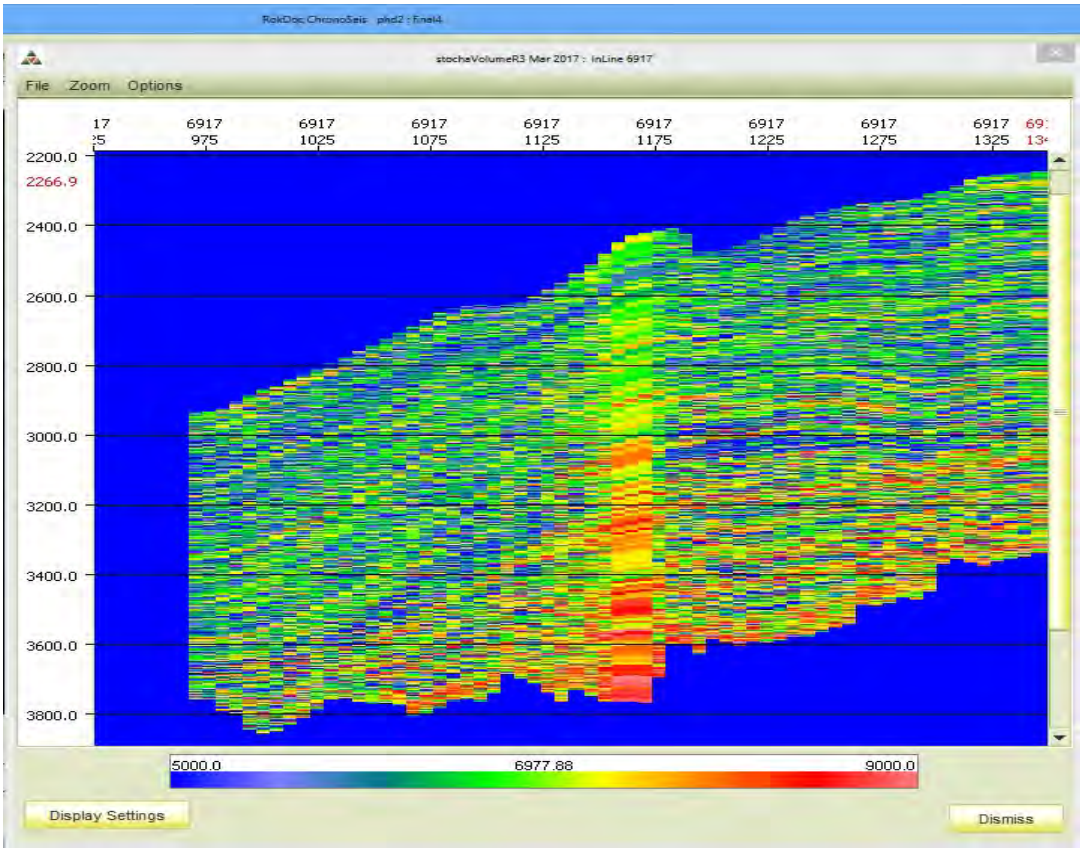


Figure 17: *3rd Realization of Stochastic Inversion on Inline 6917*

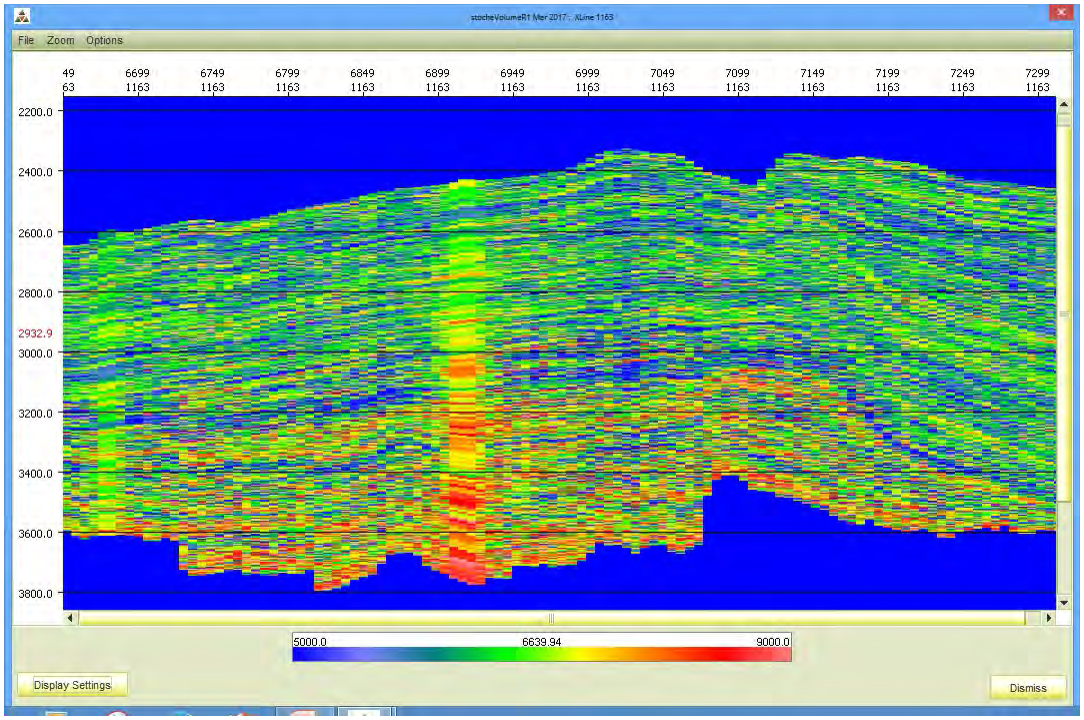


Figure 18: *1st Realization of Stochastic Inversion on Crossline 1163*

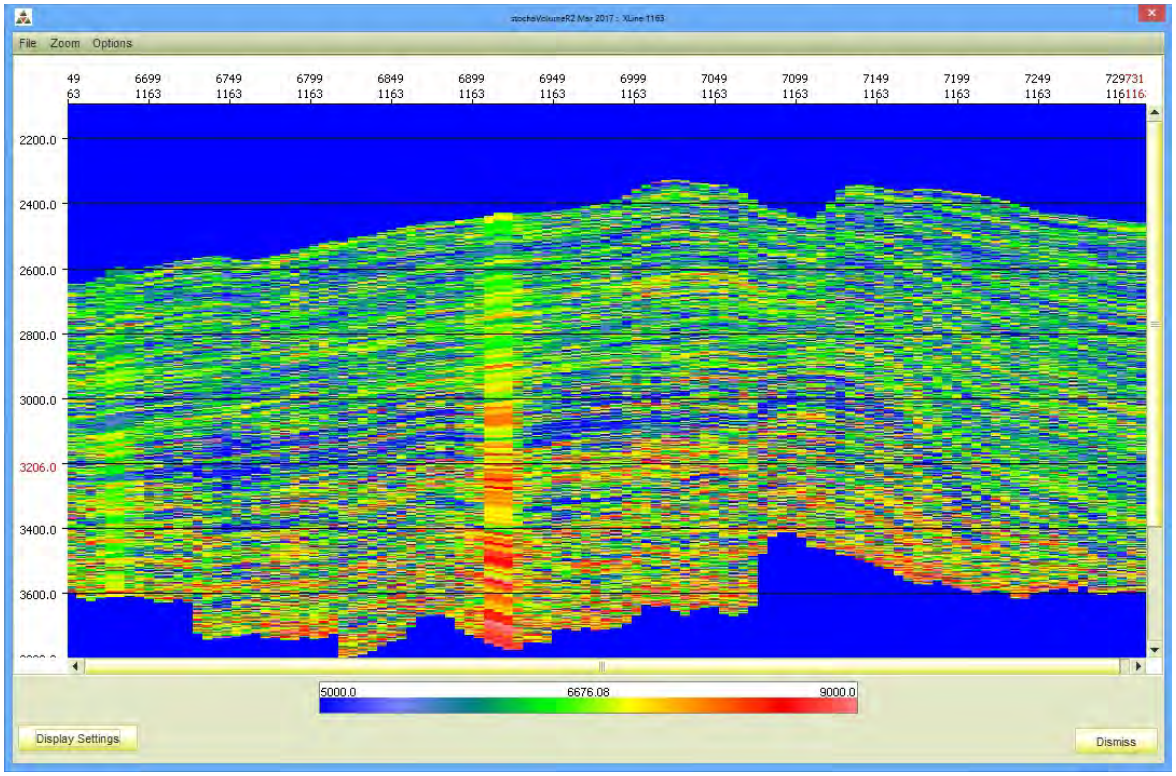


Figure 19: *2nd Realization of Stochastic Inversion on Crossline 1163*

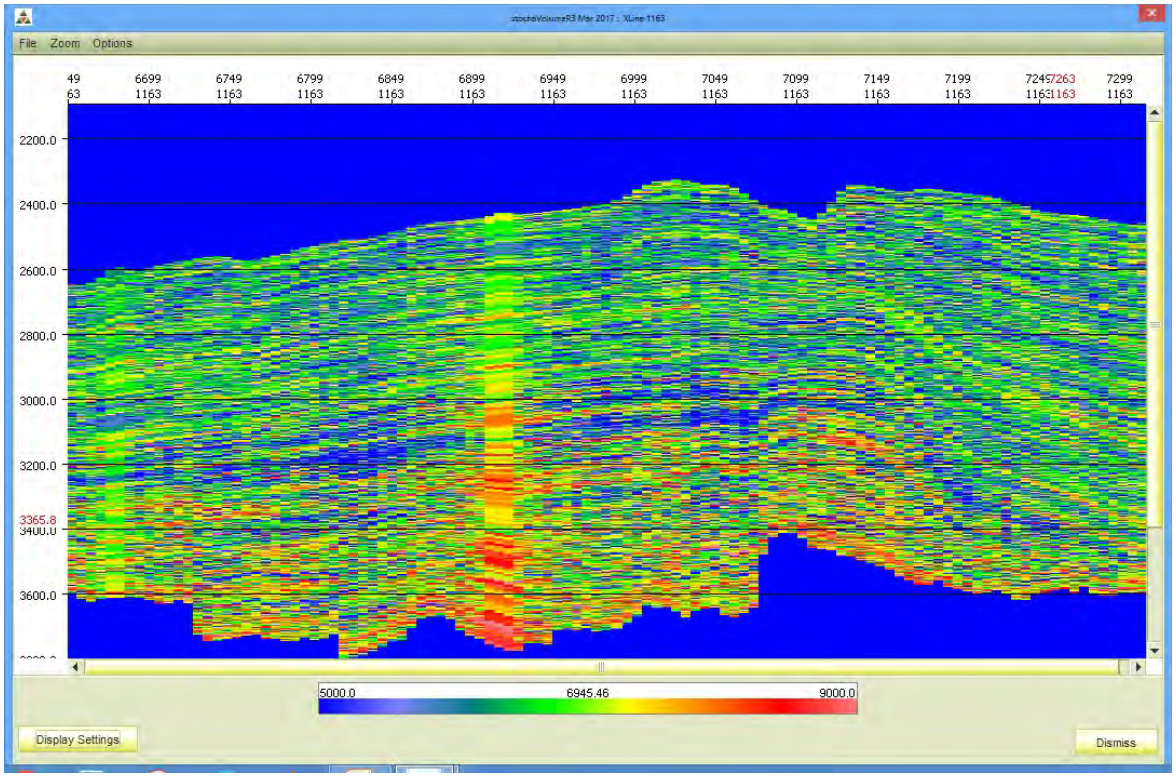


Figure 20: *3rd Realization of Stochastic Inversion on Crossline 1163*

The stochastic inversion results on crossline 1163 for the three realizations are shown in Figures 18, 19 and 20 respectively. The inversion result at the location of wells 1 and 4 are different for the three realizations. In the first realization the red colour represent higher, the green and yellow represent lower impedance values, while blue shows very low impedance values. Lower P-impedance values dominate the upper part of the section where sands 1 and 2 are located.

The impedance values between two way time 2400ms to 2800ms is from 650m/s*g/cc to 770m/s*g/cc. The high acoustic impedance values that dominate the lower part of the section could be as a result of shales and sands that are compacted by overburden pressure or the absence of fluid within it, however we have some low acoustic impedance layers within them. The acoustic impedance values at the upper part of well 4 is not as distinct as well 1 and some layers are continuous across the section, while others are not and this could be due to structural or stratigraphic changes. In the second realization of the stochastic inversion on crossline 1163, there appears to be an anticlinal structure with a higher impedance colour (red) above it to the right of well 1(center). If the structure is hydrocarbon bearing, the high impedance could be a shaly layer which can serve as a seal for the oil or gas trapped within it.

The third realization of the stochastic inversion on crossline 1163 also shows the variation in acoustic impedance on the section, the impedance values at the lower part of the section are higher than what we had in the first and second realizations. The P-Impedance value at the upper part of the section where sands 1 and 2 are located is also favourable to accommodate the presence of hydrocarbon. The anticlinal structure that was evident in the second realization is also present here with the probable sealing layer. Impedance values toward the right hand side of the section is lower, while some layers are continuous across the section, others are not. The difference in acoustic impedance distribution for the same crossline in three different realizations shows the heterogeneity that exists in the subsurface which also account for the measured uncertainties.

Conclusion

The reservoir characterization of 'Bright' field, Niger Delta using stochastic seismic inversion has been able to unravel its hydrocarbon potential. Strata models of P-Impedance , density, porosity and Vp/Vs ratio all indicate the presence of hydrocarbon within the two sand bodies mapped. The deterministic inversion sections along the structures also showed favourable impedance values within the reservoirs of interest. The three realizations of stochastic inversion sections generated shows variation in acoustic impedance on both inlines and crosslines and the acoustic impedance values at the location of Sands 1 and 2 are low; indicative of the prescence of hydrocarbon.

REFERENCES

Aleardi, M. (2018). Estimating petrophysical reservoir properties through extended elastic impedance inversion: applications to off-shore and on-shore reflection seismic data. *Journal of Geophysics and Engineering*, Vol. 15, pp. 2079–2090.

Buland, A. and Omre, H. (2003). Bayesian

linearized AVO inversion. *Geophysics*, Vol. 68, pp. 185–198.

Castagna, J. P. (2001). Recent advances in seismic lithologic analysis. *Geophysics*, Vol. 66, pp. 42–46.

Connolly, P. A. and Hughes, M. J. (2016). Stochastic inversion by matching to large numbers of pseudo-wells. *Geophysics*, Vol. 81, pp. M7–M22.

Cosentino, L. (2001). Integrated reservoir studies. *Technip*, Paris, 310p.

Doust, H., and Omatsola, E. (1990). Niger Delta, *in*, Edwards, J. D., and Santogrossi, P.A., eds., Divergent/passive Margin Basins, AAPG Memoir 48: Tulsa, *American Association of Petroleum Geologists,* pp. 239-248.

Downton, J. E. (2005). Seismic parameter estimation from AVO inversion, *PhD Thesis, University of Calgary, Alberta*, pp. 84–124.

Falebita, D. E. (2011). The Application of multiple-point stochastic inversion in reservoir characterization of 'TELDOMI' Field Niger Delta: *Ph.D. dissertation, Obafemi Awolowo University Ile Ife*. 250p.

Feng, R., Luthi, S.M. and Gisolf, D., (2018). Simulating reservoir lithologies byan actively conditioned Markov chain model. *Journal of Geophysics and Engineering*, Vol. 15, pp. 800–815.

Ghosh, S. K., Di Luca, M., Azuaje, V. Betancourt, J. G.and Del Pilar, D. (2013). Valle Inferior de Magdalena — Area Guama: Marco Estratigrafico-Sedimentológico: *Pacific Rubiales Energy, internal report,* .pp. 10-15.

González, E.F., Mukerji, T. and Mavko, G. (2008). Seismic inversion combining rock physics and multiple-point geostatistics, *Geophysics*, Vol. 73, pp. R11–R21.

Gunning, J. and Glinsky, M. E., (2004). Delivery: an open-source model-based Bayesian seismic inversion program. *Computers & Geosciences*, Vol. 30(6). pp. 8-20.

Latimer R, Davison R, van Riel P (2000). An interpreter's guide to understanding and working with seismic-derived acoustic impedance data. *The Leading Edge* Vol. 19(3), pp. 242–256

Li, K., Yin, X. and Zong, Z. (2017). Pre-stack Bayesian cascade AVA inversion in complex-Laplace domain and its application to the broadband data acquired at East China. *Journal of Petroleum Science and Engineering*, Vol. 158, pp. 751–765.

Li, K., Yin, X. and Zong, Z. (2019). Reliability enhancement of mixed-domain seismic inversion with bounding constraints. *Inverse Problems in Science and Engineering*, Vol. 27, pp. 255–277.

Moyen. R., and Doyen, P. M. (2009). Reservoir Connectivity Uncertainty from stochastic Seismic Inversion. *79th Annual International Meeting, SEG, Expanded Abstracts*, pp. 2378-2382.

Russell, B. (2005). Strata workshop: theory and exercises in seismic inversion and AVO,

unpublished lecture notes.

Russell, B. H., Hedlin, K., Hilterman, F. J. and Lines, L. R. (2003). Fluid-property discrimination with AVO: A Biot–Gassmann perspective. *Geophysics*, Vol. 68, pp. 29–39.

Russell, B. H., Gray, D. and Hampson, D. P. (2011). Linearized AVO and poroelasticity, *Geophysics*, Vol. 76, pp. C19–C29.

Schlumberger (2008) Space-adaptive inversion. Reading Between the Lines. Oilfeld Review. http://www.slb.com/content/services/seismic/reservoir/inversion/space_adaptive.asp. Accessed 22 Apr 2008

Short, K. C. and Stauble, J. (1967). Outline geology of the Niger Delta. *AAPG Bull* Vol. 5, pp. 761–779

Vazquez, R., Mendoza, A., Lopez, A., Linares, M. and Bernal, H. (1997). 3-D seismic role in the integral study of the Arcabuz-Culebra field, Mexico. *The Leading Edge*, *Vol.* 16(12), pp. 1763-1766

Veeken, P. C. H. (2007). Seismic stratigraphy, basin analysis and reservoir characterisation. (handbook of geophysical exploration). Vol. 37. xi + 509 pp. Amsterdam, Boston, Heidelberg, London

Yin, X. and Zhang, S. (2014). Bayesian inversion for effective pore-fluid bulk modulus based on fluid-matrix decoupled amplitude variation with offset approximation. *Geophysics*, Vol. 79, pp. R221–R232.

Yin, X.Y., Zong, Z.Y. and Wu G.C. (2015). Research on seismic fluid identification driven by rock physics. *Science China: Earth Sciences*, Vol. 58, pp. 159–171.

Yin, X., Li, K. and Zong Z., (2016). Resolution enhancement of robust Bayesian prestack inversion in the frequency domain, *Journal of Geophysics and Engineering*, Vol. 13, pp. 646–656.

Yin X., Zheng, Y. and Zong, Z. (2017). Research on the equivalence between digital core and rock physics models. *Journal of Geophysics and Engineering*, Vol. 14, pp. 666–674.

Zhang F., Wang, Y. and Li, X.Y. (2012). Viabilities of seismic ray impedance and elastic impedance for hydrocarbon and discrimination. *Geophysics*, Vol. 77, pp. M39–M52.

Zhang, F., (2017). Estimation of anisotropy parameters for shales based on an improved rock physics model, part 2:case study. *Journal of Geophysics and Engineering*, Vol. 14, pp. 238–254.